Robust model-based transformation and averaging of diffusion weighted images – applied to diffusion weighted atlas construction

Marc Niethammer, Yundi Shi, Sami Benzaid, Mar Sanchez, Martin Styner

UNC Chapel Hill

Abstract. This paper describes a method for model-based averaging of sets of diffusion weighted magnetic resonance images (DW-MRI) under space transformations (resulting for example from registration methods). A robust weighted least squares method is developed. Synthetic validation experiments show the improvement of the proposed estimation method in comparison to standard least squares estimation. The developed method is applied to construct an atlas of *diffusion weighted images* for a set of macaques, allowing for a more flexible representation of average diffusion information compared to standard diffusion tensor atlases.

1 Introduction

Diffusion weighted magnetic resonance imaging (DW-MRI) has become an indispensable tool for in-vivo analysis of tissue properties, in particular for brain imaging. Data analysis is typically not performed on the DW-MRIs directly, but based on diffusion tensors or derived measures. Recently, attention has shifted to more flexible representations, such as orientation distribution functions or even full directional displacement probability distributions. To analyze data in-between or across subjects the use of atlas-based methods has been tremendously successful. While atlases for structural MRI data and diffusion tensors exist, methods to construct atlases for more general descriptions of diffusion information have not been thoroughly explored, but would be of high value to allow for comprehensive data analysis. Challenges for the estimation of such atlases are: (1) the signal to noise ratio (SNR), (2) the chosen signal representation, (3) the need to account for orientation changes for orientation-dependent quantities such as diffusion tensors or the DWIs themselves, and (4) the choice of a proper registration method to compute the transformations from subject to atlas space.

While high SNR DW-MRIs can be obtained with sophisticated imaging protocols and long acquisition times, for many studies increased acquisition times are not realistic (for example when anesthesia is used and cannot be applied for an unlimited duration) and the available images are consequentially noisy. Therefore, a vast number of methods has been developed to increase signal to noise ratios. These range from simple voxel-wise averaging to technically sophisticated averaging procedures for diffusion tensors. To perform optimal averaging (from a statistical point of view), the non-Gaussian noise characteristic of DW-MRI signals should be considered. Further, the use of statistically robust estimation

methods is advisable to allow for the rejection or down-weighting of potential outliers.

Such statistically robust estimation methods have been studied for tensor estimation in [1,2,3]. This paper explores statistically robust estimation methods in the context of general parametric models taking into account an approximation to the Rician noise model. In particular, a robust variant of weighted-least-squares is investigated and applied to construct an atlas of DWIs based on a spherical harmonics expansion, which has not been investigated previously.

Diffusion information is orientation dependent, which needs to be accounted for within the atlas-building process. In the simplest case this can be accomplished by using a tensor model and reorienting the tensors according to the local deformation given by the mapping from subject to atlas space [4,5,6]. Atlas-building based on a 4th order tensor model has been proposed in [7]. In both cases, the challenge is to incorporate appropriate spatial transformations within the image-match term of the registration formulation. Instead of using the transformation of a diffusion model directly it can also be used to reconstruct DWIs for any given gradient direction. Based on this idea Tao and Miller [8] developed an image-to-image registration method by interpolating diffusion information on the sphere using a weighted average based on geodesic distances on the sphere. Yu [1] uses a robust tensor model to generate DW signals driving a registration process and Melbourne [9] addresses contrast changes for image-to-image registration by principal component modeling.

For this paper the computation of the maps from subject to atlas space (the registration) is not the focus (for the experimental section, this is accomplished through a fluid flow registration on fractional anisotropy images). Instead, it is concerned with robustly computing average DWI images from a set of images in atlas space, thereby constructing a DWI atlas. Note however, that the methods by [7,8,1,9] could easily be adapted to function as component algorithms to compute the maps to atlas space, to achieve improved alignment in particular in the areas of crossing fibers.

Sec. 2 discusses DWI noise models. Sec. 3 introduces the general robust M-estimation framework for DW measurements. Secs. 3.1 and 3.2 discuss the estimation of individual signals and parametric signal profiles respectively. Sec. 4 highlights applications to registration and atlas-building. Results for the construction of a diffusion-weighted atlas are shown in Sec. 5.

2 Noise Modeling

Measured diffusion weighted images are assumed to follow a Rician noise distribution with probability density function [10]

$$p(S_i) = \frac{S_i}{\sigma_i^2} e^{-\frac{S_i^2 + (S_i^n)^2}{2\sigma_i^2}} I_0\left(\frac{S_i S_i^n}{\sigma_i^2}\right), \tag{1}$$

where S_i is the measured (noisy) signal, S_i^n is the true signal, σ_i^2 is the noise variance, and I_0 the modified Bessel function of order 0. Given a set of measure-

ments $\{S_i\}$ and a signal model (tensor, spherical harmonics expansion, etc.), the maximum likelihood (ML) estimators can be formulated and solved numerically.

The log-transformed random variables S_i can be approximated as Gaussian distributed random variables with a signal-dependent variance [10], i.e.,

$$\log(S_i) \approx \log(S_i^n) + \epsilon_i, \quad \epsilon_i \sim N\left(0, \frac{\sigma_i^2}{(S_i^n)^2}\right), \tag{2}$$

where $N(\mu, \sigma^2)$ denotes a normal distribution with mean μ and variance σ^2. This is an excellent approximation for reasonably high signal to noise ratios; see [10] and Fig. 1. This relation can be exploited for the estimation of any parametric model. Typically, σ_i is assumed constant, since noise in the DWIs is expected to be constant. However (see Sec. 5), this assumption is problematic for robust estimators and bias field correction should be applied to DWIs to equalize noise levels.

3 Robust estimation of diffusion weighted signals

Least squares (LS) estimation for signals derived from log-transformed DWIs is simple, approximates the Rician noise model well for moderate and large signal amplitudes (when using weighted least squares) and is still predominantly used in practice. Due to the Gaussian noise model in the log-domain, it is easy to make use of robust M-estimation methods, where a model residual is penalized by a non-quadratic loss function. The benefits of such an approach have been demonstrated for tensor estimation [2,3]. This paper investigates robust signal estimation for general parametric models from sets of DWIs. This includes simple signal averages (for repeated measurements) as well as the coefficient estimation for series expansions of diffusion profiles (e.g., spherical harmonics expansion), where statistically robust methods have so far not been applied. (Note that methods have been developed [11,12] which impose a certain level of smoothness and therefore show decreased sensitivity to noise and improved reconstruction quality. However, the notion of robustness in [11,12] is different from the one used in this paper, which addresses outliers and can be combined with a smoothness assumption as a prior on the parametric model.)

To avoid explicitly identifying (and rejecting) outliers, outliers can be down-weighted by an appropriate choice of loss function $\rho(u)$. In general, given a model parametrized by coefficients $\boldsymbol{c}$, M-estimation [13,14] amounts to minimizing

$$E(\boldsymbol{c}) = \sum_{i=1}^{N} \rho\left(\frac{r_{i,\boldsymbol{c}}}{v_i}\right), \tag{3}$$

where $r_{i,\boldsymbol{c}}$ is the residual measuring the difference between the i-th measurement and the chosen model, and v_i is a possibly signal-dependent scale factor. The loss function $\rho(u) = \frac{1}{2}u^2$ recovers LS optimization. The optimality condition is

$$\frac{dE(\boldsymbol{c})}{d\boldsymbol{c}} = \sum_{i=1}^{N} w\left(\frac{r_{i,\boldsymbol{c}}}{v_i}\right) \frac{1}{v_i^2} \frac{dr_{i,\boldsymbol{c}}}{d\boldsymbol{c}} r_{i,\boldsymbol{c}} = 0, \tag{4}$$

where $w(u) = \frac{1}{u}\frac{d\rho(u)}{du}$ is called the weight function. For the special case of the quadratic loss function, $w(u) = 1$; choosing $\frac{1}{v_i^2} = \frac{(S_i^n)^2}{\sigma^2}$ results in the weighted least squares problem for diffusion weighted images, where σ is the noise variance in the diffusion weighted signals (assumed constant) and a parameter of the Rician distribution. For the experiments in this paper this parameter is estimated from a baseline image [15]. Thus, robust M-estimation for DWIs can be written in general as

$$E(\boldsymbol{c}) = \sum_{i=1}^{N} \rho\left(\frac{S_i^n r_{i,\boldsymbol{c}}}{\sigma}\right). \tag{5}$$

Operating on log-transformed signals is essential for the weighted LS approximation to the Rician noise model and fits nicely into the M-estimation framework.

Choosing $r_{i,\log S^n} = \log S_i - \log S_i^n$ (where $S_i^n = S^n$ is a constant) and $r_{i,\{\log S_0^n, D\}} = \log S_i - \log S_0^n + \frac{1}{b} g_i^T D g_i$ (with $\log S_i^n = \log S_0^n - \frac{1}{b} g_i^T D g_i$) results in estimators for a single signal S^n and for the baseline image S_0^n and the diffusion tensor D respectively. (Note that in the absence of the nominal value S_i^n, its value is chosen according to the parametric model.) Other parametric models may be chosen, e.g.,

$$r_{i,\boldsymbol{c}} = \log S_i - \sum_{j=1}^{R} c_j Y_j(\theta_i, \phi_i) \tag{6}$$

where $\{Y_j(\theta, \phi)\}$ define a model-basis on the sphere. Any spherical basis – not necessarily restricted to a spherical shell – fits into this estimation framework.

In what follows, measurements are assumed to be either baseline images (with no diffusion weighting) or have gradients distributed on a spherical shell (i.e., for a fixed b value). While a multitude of robust loss functions have been proposed, the remainder of the paper focuses on the Huber function

$$\rho(u) = \begin{cases} \frac{1}{2}u^2, & |u| \le \theta, \\ \frac{1}{2}\theta\left(2|u| - \theta\right), & |u| > \theta, \end{cases}, \quad w(u) = \begin{cases} 1, & |u| \le \theta \\ \frac{\theta}{|u|}, & |u| > \theta \end{cases} \tag{7}$$

since it is quadratic for $u \le \theta$. Therefore the minimizer to Eq. 5 recovers the optimal weighted least-squares solution for small residuals and down-weights potential outliers with larger residuals. In Eq. 7, θ is a design parameter. Since the scale parameter standardizes the residuals with $\frac{S_i^n}{\sigma}$ (according to the weighted least squares approximation for the Rician noise model), fixing θ specifies the transitioning point between a quadratic and a absolute difference penalizer at θ times the expected standard deviation of the residuals. (For all experiments in this paper: $\theta = 2$). Such a down-weighting of a residual's influence with residual magnitude is a fundamental property of robust M-estimators to diminish the effect of potential outliers (for example: using a quadratic loss function to estimate a central element for a set of real numbers recovers the mean, while using the magnitude function recovers the median). In fact, loss-functions such as the truncated quadratic function can also be used which disregard values above a certain residual threshold in the estimation process (where the weighting function w becomes zero).

3.1 Averaging of corresponding diffusion weighted images

The signal underlying a set of corresponding diffusion weighted images $\{S_i\}$ (which correspond to the same gradient direction and are expected to be drawn from the same distribution) can be reconstructed, assuming the Gaussian model with mean-dependent variance, by minimizing Eq. 5 with $r_{,\log S^n} = \log S_i - \log S^n$. This is useful for the averaging of sets of baseline images which do not change contrast under space transformations. Assuming a given, identical variance for all measurements, the solution to the optimization problem is

$$S^n = e^{\frac{1}{n}\sum_{i=1}^{n}\log S_i} = \prod_{i=1}^{n}(S_i)^{\frac{1}{n}},$$

which is the geometric mean of the measured values. The robust version using the Huber function can be solved by iterating

$$(S^n) \leftarrow \prod_{i=1}^{n}(S_i)^{\frac{w_i}{W}}, \quad W = \sum_{i=1}^{n} w_i, \quad w_i = w\left(\frac{S^n(\log S_i - \log S^n)}{\sigma}\right)\left(\frac{S^n}{\sigma}\right)^2$$

to convergence. Note that this is not an ML estimate under the assumed noise model, but rather a pseudo ML estimate [16], where the signal variance is estimated or known. It is easy to compute and results in significantly improved signal estimation quality over arithmetic averaging as demonstrated in Figs. 1 and 2. Estimation quality is comparable to the one for the maximum-likelihood estimator using the Rician noise model for large and moderately large signal values. Further, the robust estimator outperforms the non-robust variants when outliers are present. This motivates using the robust weighted approach for the estimation of more general diffusion profiles.

3.2 Estimation of diffusion profiles

Given a basis for signal representation on the sphere with the residual defined as in Eq. 6 (for example spherical harmonics) the same iterative reweighting process as for the estimation of corresponding DWIs of Sec. 3.1 can be applied for the estimation of the series coefficients, $\boldsymbol{c}$. The robust estimation model is given in Eq. 5. Working in the log-transformed domain also has the benefit that the overall estimated signal (obtained by exponentiation) is assured to be positive, which is physically meaningful. Arguably, the fitting domain should be irrelevant if the correct noise model for the respective signal representation is used. Regularized solutions are obtained by penalizing basis coefficients

$$E(\boldsymbol{c}) = \boldsymbol{c}^T L \boldsymbol{c} + \sum_{i=1}^{N} \rho\left(\frac{S_i^n r_{i,\boldsymbol{c}}}{\sigma}\right). \tag{8}$$

For spherical harmonics the regularization matrix L can be chosen such that it results in smoothing of the reconstructed signal on the spherical shell (according

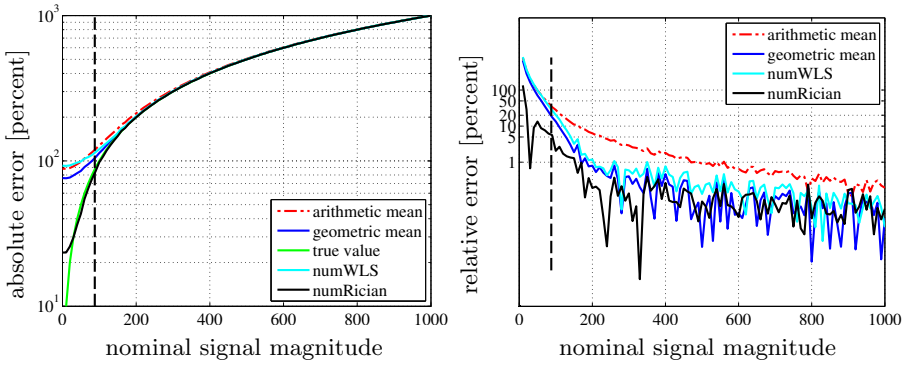

Fig. 1. Absolute (left) and relative error (in percent; right) for estimating a nominal diffusion weighted signal at various signal intensity levels for a noise level $\sigma = 70$. Estimations were obtained using the arithmetic mean, the geometric mean (pseudo-maximum-likelihood), the weighted least squares maximum-likelihood (ML) estimator (WLS) and through estimation by the Rician ML estimator. Each value represents the average of the estimation errors for 1,000 runs using ten independent measurements corrupted with Rician noise. The vertical dashed line indicates the mean for Rayleigh noise $\mu = \sqrt{\frac{\pi}{2}}\sigma$, ie., what the expected intensity value would be in the presence of a zero signal. The Rician ML estimator is superior to all other estimator for very low signal values. However, the simple geometric mean performs well for moderate to high signal values. The arithmetic mean shows the worst performance.

to the Laplace-Beltrami smoothing operator) as described in Descoteaux [11]. Note that the energy balance between prior and data likelihood changes for large numbers of measurements. Therefore, for a fixed model order the influence of the prior decreases with an increase in measurements and the estimator converges to the ML estimator in the limit. This is a standard property of the MAP estimator and highly useful for example for DWI atlas building (see Sec. 4), where large numbers of images are averaged and a prior is no longer urgently needed.

The performance of the robust estimation method for a real, symmetric spherical harmonics basis is demonstrated for two example diffusion profiles (crossing and non-crossing) in comparison to fitting the signal through LS in the original domain and in the log-transformed domain respectively (see Tabels 1 and 2). The robust weighted approach outperforms the two other methods, in particular when the number of measurements is large in comparison to the model order.

4 Application to registration and DW atlas-building

While methods for diffusion tensor (DT) [6] and higher-order tensor [7] atlas-building have been developed, methods for the computation of DW atlases have not been explored. This paper is not concerned with developing a new way of computing the space transformations from subject to atlas space, but instead

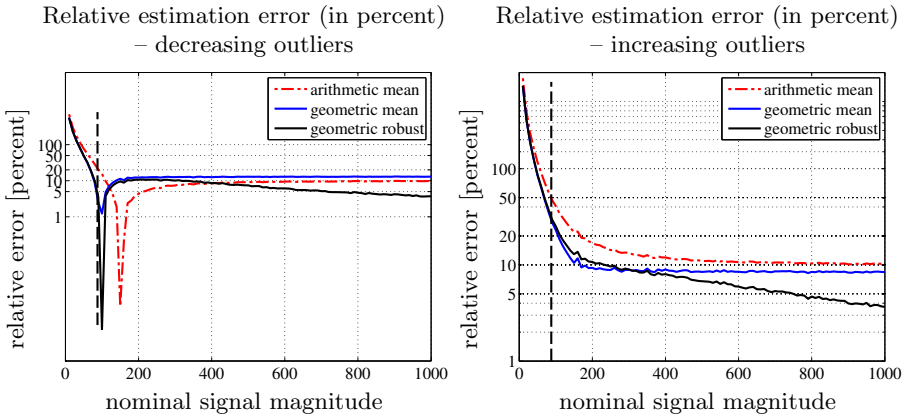

Fig. 2. Relative estimation error for the robust estimation method using the Huber function with $\theta = 2$. Each value represents the average of the estimation errors for 1,000 runs using ten independent measurements corrupted with Rician noise. For each set of ten measurements two were randomly chosen and their value was decreased by 50% (left) or increased by 50% (a similar outlier-creation strategy as in [2]). The robust geometric mean shows greatly improved performance for increasing outliers. It performs better than the geometric mean for decreasing outliers and also shows improved performance for larger values in comparison to the arithmetic mean. Presumably this can be explained by the large expected signal variations for low signal values, which makes outlier rejection more difficult in these cases. Further the estimation error shows dips only for the case of outliers decreasing signal magnitude. Presumably this is due to the fact that the estimators in general tend to overestimate signal magnitude and therefore at certain values the outliers can have a seemingly beneficial effect. (In fact the dips shift to the left with stronger signal drops – not shown in this figure.)

makes use of the transformations to compute a new average set of DWIs for a canonical set of gradient directions. The atlas-building strategy used for the experimental results in Sec. 5 is due to Joshi et al. [17]. Here, a greedy approach is used to obtain the set of space transformations, $\{\Phi^i\}$ and the average atlas image I^T approximately minimizing the energy

$$E(I^T, I^i) = \sum_{i=1}^{N} \left(\int_0^1 \|v^i\|_L^2 \, dt + \|I^T - I^i(1)\|_{L_2}^2 \right),$$

$$\text{such that} \quad (I^i)_t + \nabla I^i \cdot v^i = 0, \quad I^i(0) = I_0^i,$$

where I^T denotes the atlas image, $I^i(t)$ the subject image transformed for time t through the velocity field v^i and L is a differential operator to ensure smoothness of the transformations. The maps from subject to atlas space can be computed for each subject i by solving $\Phi_t^i + D\Phi^i v^i = 0$; $\Phi^i(0) = id$, where id denotes the identity map and D the Jacobian. For the experiments in this paper, $\{I^i\}$

		Gradient scheme and estimation method					
		46 dir			181 dir		
rel. error [percent]		SHO-2	SHO-4	SHO-8	SHO-2	SHO-4	SHO-8
	0	6.2/14.2/**4.7**	7.8/11.5/**6.2**	10.0/12.5/**8.9**	3.3/13.6/**2.5**	4.0/9.4/**3.2**	5.3/8.8/**4.5**
	10↑	9.7/13.7/**8.4**	10.2/13.7/**9.0**	11.7/14.6/**10.7**	5.3/10.5/**4.4**	5.6/10.2/**4.7**	6.5/10.5/**5.5**
	20↑	11.6/15.4/**10.5**	12.0/15.6/**11.0**	13.2/16.4/**12.3**	6.8/11.7/**5.7**	7.2/11.9/**6.1**	7.9/12.4/**6.9**
	30↑	13.4/17.2/**12.4**	13.8/17.6/**13.0**	14.9/18.4/**14.2**	8.5/13.4/**7.3**	9.0/13.9/**7.8**	9.6/14.4/**8.6**
	10↓	10.0/13.0/**8.5**	10.7/12.9/**9.0**	12.0/13.8/**10.8**	5.8/9.9/**4.5**	6.3/9.3/**4.7**	7.2/9.5/**5.5**
	20↓	12.2/14.0/**10.7**	12.8/14.2/**11.3**	13.8/15.0/**12.4**	7.8/10.1/**5.9**	8.6/10.2/**6.4**	9.4/10.5/**7.2**
	30↓	14.3/15.3/**12.9**	14.9/15.7/**13.5**	15.8/16.4/**14.5**	10.3/11.1/**7.9**	11.0/11.4/**8.5**	11.8/11.9/**9.3**

Table 1. Estimation results for a diffusion model of the form $S_k = S_0(0.2e^{-bd} + 0.8e^{-bdg_k^T Ag_k}$, with $S_0 = 1000$, $b = 1000$, $d = 0.002$, $A = e_1e_1^T$, where $e_1 = (1, 0, 0)^T$. Gradient directions were obtained by constructing icosadeltahedra with 92 and 362 vertices through the electric repulsion model, with antipodal pairs removed to result in gradient schemes with 46 and 181 directions respectively. Results are tabulated for different orders of the spherical harmonics expansion (2, 4, 8) and for different percentages of outliers (0, 10, 20, 30), where outliers were generated by increasing ↑ or decreasing ↓ their value by 50%. Rician noise of $\sigma = 70$ was added to all measurements. Results are tabulated as a/b/c, where: a=LS in log-transformed domain; b=LS in original signal domain; c=robust weighted LS in log-domain. Results represent the mean relative errors for all gradient directions averaged over 1,000 random experiments in percent. The robust WLS method (described in this paper) outperforms the two other methods.

		Gradient scheme and estimation method					
		46 dir			181 dir		
rel. error [percent]		SHO-2	SHO-4	SHO-8	SHO-2	SHO-4	SHO-8
	0	8.0/8.1/**7.9**	7.6/7.5/**7.3**	8.9/9.0/**8.8**	**7.0**/7.3/7.1	5.3/5.5/**5.2**	5.6/5.7/**5.5**
	10↑	9.2/9.5/**9.0**	9.4/9.9/**9.2**	10.5/10.9/**10.4**	6.3/6.6/**6.1**	6.2/6.8/**5.9**	6.6/7.3/**6.3**
	20↑	10.8/11.4/**10.5**	11.0/11.9/**10.9**	12.0/12.7/**11.8**	7.2/8.1/**6.8**	7.5/8.6/**7.0**	8.0/9.2/**7.5**
	30↑	12.4/13.4/**12.2**	12.8/13.9/**12.7**	13.7/14.8/**13.6**	8.6/10.0/**8.1**	9.0/10.6/**8.5**	9.6/11.2/**9.1**
	10↓	9.5/9.1/**8.9**	10.0/9.3/**9.1**	11.0/10.4/**10.2**	6.4/6.2/**5.9**	6.7/6.1/**5.8**	7.3/6.6/**6.3**
	20↓	11.5/10.6/**10.4**	12.0/10.9/**10.8**	12.8/11.9/**11.8**	8.2/7.1/**6.7**	8.8/7.4/**7.0**	9,4/8.0/**7.6**
	30↓	13.5/**12.2**/**12.2**	14.1/**12.7**/12.8	14.9/**13.6**/13.7	10.3/8.6/**8.3**	11.1/9.1/**8.8**	11.8/**9.6**/**9.6**

Table 2. Estimation results for a two-tensor diffusion model of the form $S_k = S_0(0.2e^{-bd} + 0.4e^{-bdg_k^T Ag_k} + 0.4e^{-bdg_k^T Bg_k})$, with $b = 1000$, $S_0 = 1000$, $d = 0.002$. A and B where constructed as the outer product of two vectors at an angle of 70 degrees. Table information is organized in the same way as in Table 1. The robust method performs best in almost all cases.

denotes the set of FA images for the subjects. Note that any other atlas-building strategy for diffusion weighted images can be used to obtain the set of space transformations from subject to atlas space. In particular, registration strategies using orientation information within the image similarity measure could be useful [7,8,1,9,18,19] as components for the atlas building.

As in DT atlas building, DW atlas-building requires signal transformation and signal averaging. This can either be done by model fitting in the original image domain followed by transformation and averaging of the model coefficients

or by adjusting the B-matrix according to the space transformation as discussed in [5]. Based on the model fitting and averaging method outlined in the previous section, this paper follows the latter approach.

While for affine transformations the measurement frame can be adjusted globally, doing so in the context of non-rigid registration would require local adjustments of measurement frames and prohibitive storage space for large numbers of images. Therefore, an estimation of the DWIs in the transformed space for a given set of gradient directions is useful. This can be accomplished by locally reorienting the gradient directions $\{g_i\}^j$ for all j original images in atlas space, based on the space transformations [4]. The associated signal intensities $\{S_i\}^j$ are kept fixed. Given the set of associated rotations $\{R^j\}$, the new compound signal is

$$\bigcup_j \{R^j g_i\}^j, \quad \text{with signals} \quad \bigcup_j \{S_i\}^j.$$

Computing the series coefficients for a robust approximation of the compound signal results in a continuous parametric function which can be evaluated for any desired gradient direction. This allows resampling for a set of canonical gradient directions and can be used for atlas-building with any chosen parametric model. Fig. 3 illustrates this principle as used in Sec. 5 to build a diffusion weighted atlas.

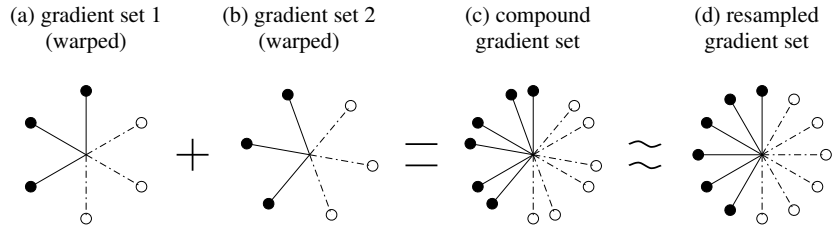

Fig. 3. Principle of gradient warp to obtain resampled DWIs illustrated by two exemplary sets of gradient directions. Solid and dashed lines denote antipodal pairs for gradient directions. Gradient directions are typically identical before transformation to atlas space. Given space transformations to atlas space the gradient directions are locally rotated consistent with the local spatial rotation induced by the transformation maps (a,b). The DWI values stay fixed, but the full set of measurements is attributed to a new compound set of gradients (c). Since nonlinear space transformations are to be supported the profile of DWI values are resampled (in the ADC domain) based on a robust model fit using spherical harmonics to yield a set of DWIs with a chosen, canonical set of gradient directions valid for the full atlas space (d).

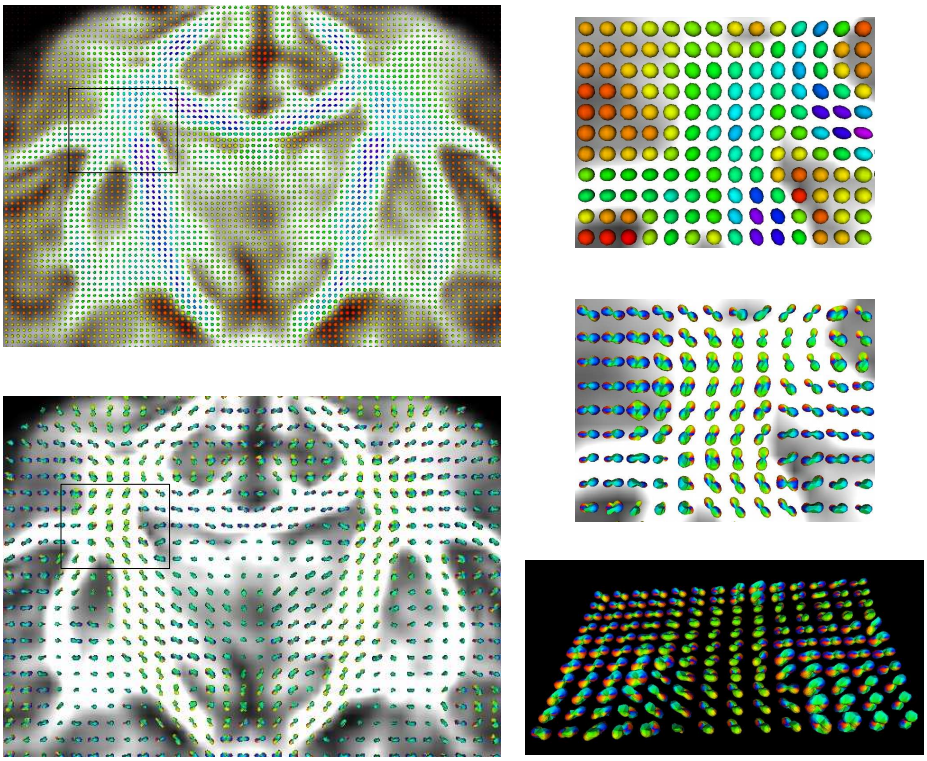

Fig. 4. Coronal brain slice with ODF and tensor ellipsoids overlaid on an FA image. The ROI where the fibers from internal capsule and corpus callosum are expected to cross is marked. Right: tensor ellipsoids (top) and ODF (middle and bottom, with two different viewing angles) shown for this ROI. ODFs reconstructed from the DWI atlas demonstrate complex fiber structure while tensor ellipsoids from the tensor atlas show very limited information.

Fig. 5. Effect of bias field on residuals. Signal intensity increases with the number of residuals above the Huber threshold $\theta = 2$. Without bias-field correction (left) and with bias-field correction (right). Bias-field correction removes most of the asymmetry.

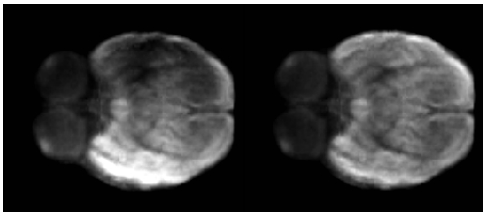

5 Diffusion Weighted Atlas-building Results

Ten rhesus monkeys of age 6 months were scanned on a 3T Siemens Trio scanner with 8-channel phase array trans-receiving volume coil. DWIs were acquired with: voxel size: $1.3\times1.3\times1.3mm^3$ with zero gap, 60 directions, TR/TE=5000/86

ms, 40 slices, FOV: 83 mm, b:0, 1000 s/mm^2, 12 averages. DWIs were up-interpolated to 0.65 mm^3 isotropic using windowed sinc interpolation. Tensors were calculated using WLS. Fractional anisotropy (FA) maps were used to construct an unbiased deformable atlas [17]. The diffeomorphic map for each individual FA to the atlas was used to warp the tensors [4] and to transform the DWIs for each subject. Warped tensor fields were averaged in the log-Euclidean space to generate the tensor atlas. The DWI atlas was computed using the robust WLS method using an 8th order symmetric spherical harmonics (SH) basis for the gradient directions and independently the robust WLS method for the baseline image.

To robustly fit the compound model of Sec. 4, requires fixing a scale parameter. For the Huber function model, the noise variance σ and the cut-off value θ need to be determined. To assure that σ is constant across the images DWIs should be bias corrected. Otherwise the outlier detection may produce inconsistent results (see Fig. 4). Note that for standard LS fitting bias field correction is typically not necessary for DWIs, because the quantities of interest are either ratios (as in DTI) or the weight function is scale-independent.

Orientation distribution functions (ODFs) were computed from the DWI atlas using 8th order SHs [11]. Fig. 4 shows the comparison between tensor ellipsoids and ODFs in a region where fibers running along the corpus callosum meet the internal capsule and the corticospinal tracts. ODFs show complex fiber structure possibly due to fiber crossing and branching, which is consistent with previous studies [11]. This information is not preserved with the tensor approach. In particular, Fig. 4 also shows that the DWI atlas successfully preserves directional information.

6 Conclusions

This paper proposed robust estimation methods for parametric models based on DWIs. Estimation is performed in the log-transformed space to exploit the approximation of the Rician noise model by a Gaussian with signal-dependent variance. By applying the estimation method to registered DWIs a DW-atlas was constructed. This allows for the representation of average diffusion information with more flexible diffusion models than the diffusion tensor. While the method was demonstrated for a one shell acquisition scheme, it could be extended to atlas-building for multi-shell acquisitions. Future work (1) will explore the effects of different basis functions on the representation of diffusion measures under the resampling step, (2) will perform atlas-building for larger numbers of subjects and for acquisitions with higher b-values to investigate the preservation of crossings for DWI atlases, and (3) will use advanced atlas-building methods which incorporate directional information with a statistically robust image similarity term to possibly improve alignment results. The software will be available in open source form.

References

1. Yu, B.: Correcting for Motion between Acquisitions in Diffusion MR. PhD thesis, University College London (2009)
2. Chang, L.C., Jones, D.K., Pierpaoli, C.: RESTORE: Robust estimations of tensors by outlier rejection. Magnetic Resonance in Medicine **53** (2005) 1088–1095
3. Mangin, J., Poupon, C., Clark, C., Le Bihan, D., Bloch, I.: Distortion correction and robust tensor estimation for MR diffusion imaging. Medical Image Analysis **6**(3) (2002) 191–198
4. Alexander, D., Pierpaoli, C., Basser, P., Gee, J.: Spatial transformations of diffusion tensor magnetic resonance images. IEEE Transactions on Medical Imaging **20**(11) (2001) 1131–1139
5. Leemans, A., Jones, D.: The B-matrix must be rotated when correcting for subject motion in DTI data. Magnetic Resonance in Medicine (2009)
6. Goodlett, C., Davis, B., Jean, R., Gilmore, J., Gerig, G.: Improved correspondence for DTI population studies via unbiased atlas building. Lecture Notes in Computer Science **4191** (2006) 260–267
7. Barmpoutis, A., Vemuri, B.C.: Groupwise registration and atlas construction of 4th-order tensor fields using the R+ Riemannian metric. In: Proceedings of MICCAI. (2009) 640–647
8. Tao, X., Miller, J.: A method for registering diffusion weighted magnetic resonance images. Lecture Notes in Computer Science **4191** (2006) 594
9. Melbourne, A.: Alignment of Conrast Enhanced Medical Images. PhD thesis, University College London (2009)
10. Salvador, R., Pena, A., Menon, D.K., Carpenter, T.A., Pickard, J.D., Bullmore, E.T.: Formal characterization and extension of the linearized diffusion tensor model. Human Brain Mapping **24** (2005) 144–155
11. Descoteaux, M., Angelino, E., Fitzgibbons, S., Deriche, R.: Regularized, fast, and robust anaytical q-ball imaging. Magnetic Resonance in Medicine **58** (2007) 497–510
12. Clarke, R.A., Scifo, P., Rizzo, G., Dell'Acqua, F., Scotti, G., Fazio, F.: Noise Correction on Rician Distributed Data for Fibre Orientation Estimators. IEEE Transactions on Medical Imaging **27**(9) (2008) 1242–1251
13. Stewart, C.V.: Robust parameter estimation in computer vision. SIAM Review **41**(3) (1999) 513–537
14. Rousseeuw, P.J., Leroy, A.M.: Robust regression and outlier detection. Wiley (1987)
15. Aja-Fernández, S., Niethammer, M., Kubicki, M., Shenton, M., Westin, C.: Restoration of DWI data using a Rician LMMSE estimator. IEEE transactions on Medical Imaging **27**(10) (2008) 1389–1403
16. Carroll, R.J., Wu, C.F.J., Ruppert, D.: The effect of estimating weights in weighted least squares. Journal of the American Statistical Association **83**(404) (1988) 1045–1054
17. Joshi, S., Davis, B., Jomier, M., Gerig, G.: Unbiased diffeomorphic atlas construction for computational anatomy. NeuroImage **23**(Supplement 1) (2004) S151 – S160 Mathematics in Brain Imaging.
18. Alexander, D.C., Gee, J.C.: Elastic matching of diffusion tensor images. Computer Vision and Image Understanding **77**(9) (2000) 233–250
19. Ruiz-Alzola, J., Westin, C.F., Warfield, S.K., Alberola, C., Maier, S.E., Kikinis, R.: Nonrigid registration of 3d tensor medical data. Medical Image Analysis **6**(2) (2002) 143–161